Using the Cellometer Vision Image Cytometer for Immunophenotyping

WHITE PAPER

Nexcelom Bioscience LLC. | 360 Merrimack Street, Building 9 | Lawrence, MA 01843
T: 978.327.5340 | F: 978.327.5341 | E: info@nexcelom.com | www.nexcelom.com

1001275 Rev. A

Using the Cellometer Vision Image Cytometer for Immunophenotyping

Introduction

Cell phenotyping through the identification of biomarkers is essential for the diagnosis of hematologic malignancy, sub-classifying diseases, monitoring response to treatment, predicting prognosis, as well as detecting rare cell populations and residual malignant cells [1-4]. In immunological study, cell surface markers have been widely used to identify and classify various immune cells and track their developmental status as well as physiological functions [5, 6].

Recently, a small desktop imaging cytometry system (Cellometer Vision) has been developed by Nexcelom Bioscience LLC for automated bright-field (BR) and fluorescent (FL) imaging methods [7]. The system can perform rapid cell enumeration and other fluorescent measurements using disposable counting slides. The software utilizes a novel counting algorithm for accurate and consistent measurements on a variety of cell types [8].

By developing fluorescent-based assays to immunophenotype cells, the Cellometer imaging cytometry can provide a quick, simple, and inexpensive alternative for biomedical research, which may be beneficial for smaller research laboratories and clinics. In this publication, we demonstrate an immunophenotyping assay to detect percentages of lymphocyte populations in the spleen and thumus via cell surface markers CD4, CD8, B220, and CD5 with Cellometer imaging cytometry as an alternative to flow cytometry. The data obtained by Cellometer were compared to those from conventional flow cytometry methods.

Materials and Methods

Cellometer Vision and Disposable Counting Chamber

The Cellometer Vision utilizes one bright-field and two fluorescent channels to perform image-based cytometric analysis. Bright-field imaging used a broadband white light-emitting diode (LED) and fluorescence imaging used three different monochromatic LEDs (470, 527, and 630 nm) as the excitation light sources. Each monochromatic excitation was paired with a specific excitation (nm)/emission (nm) filter set (475/ 525, 475/595, 527/595, and 630/695) with a bandwidth of approximately 40 nm.

Cellometer systems were designed to specifically analyze Nexcelom's disposable counting chamber, which holds precisely 20 μL of sample. Four separate areas (~1 μL) were imaged and analyzed sequentially by the system, where the target cells were identified and counted by the software. In general, combined image acquisition and cell counting time was approximately 30 seconds.

Filter sets 475/525, 527/595, and 630/695 were used in the immunophenotyping assay. The Cellometer software used a proprietary algorithm to analyze the captured bright-field and fluorescent images. Parameters such as cell circularity and size were gated to count specific population of cells from the bright-field images. Aggregation of cells was included in the total cell count by the use of declustering function, which could distinguish and count individual cells in the cluster. Fluorescent intensity within individually counted cells was measured with sample-dependent fluorescent threshold, based on which a histogram plot was generated to show distribution of fluorescent intensity in the population. Counting and fluorescence measurements were directly exported to FCS Express (De Novo Software) for flexible graph generation. Exported data file contained the number, size, and fluorescence intensity of individually counted cells.

Cell Preparation for Immunophenotyping

Lymphocytes were prepared from the spleen and thymus of BALB/c mice. Each thymus lobe was rinsed with phosphate buffered saline to remove any residual red blood cells. Thymic lobes were then gently dissociated and passed a cell strainer. Cold RPMI medium was added and single cell suspension was removed by gentle pipetting. Spleens were cut into two pieces and single cell suspension was prepared using cell strainer as described above. Erythrocytes were depleted using erythrocyte lysis buffer according to the manufacturer's instruction. Cells were then left in RPMI until use. All animal uses were performed according to institutional guidelines and approved by the IACUC at the Boston University Medical Center.

Prepared cells were then washed with PBS followed by FcR blockade with 2.4G2 anti-CD16/CD32 antibodies. For multiple-fluorescent labeling, cell surface markers on splenocytes and thymocytes were stained with R- Phycoerythrin (R-PE)-conjugated anti-mouse CD8 mAb and Biotinylated anti-mouse CD4 mAb simultaneously followed by streptavidin-conjugated APC. For single-staining controls, cell surface markers on splenocytes were stained with Fluorescein (FITC)-conjugated anti-mouse CD5 mAb, R-PE-conjugated anti-mouse CD4/ CD8 mAb, and Biotinylated anti-mouse B220 mAb, respectively, and followed by streptavidin-conjugated Allophycocyanin (APC). In addition, unstained control samples were prepared without any surface marker labels. Cells were stained with primary antibodies 45 minutes followed by two washes and fixation in formaldehyde in the FACS staining buffer. Final concentrations of fluorophore-labeled CD4, CD8, CD5, and B220 were 1, 1, 2, and 2 μg/mL, respectively.

Results

Figure 1. Detection of single-fluorescence labeling of splenocytes.

Splenocytes were stained with fluorescence-labeled antibodies, (a) anti-CD5-FITC, (b) anti-CD4/CD8-PE, and (c) anti-B220-APC. Bright-field and fluorescent images were shown.

- (d) Scatter plot of dual labeling of CD4/CD8 in respect to B220 was shown, which was consistent with the single-fluorescence plots.
- For immunophenotyping, the differences between data the obtained from Cellometer and flow cytometry were within a 5% range.

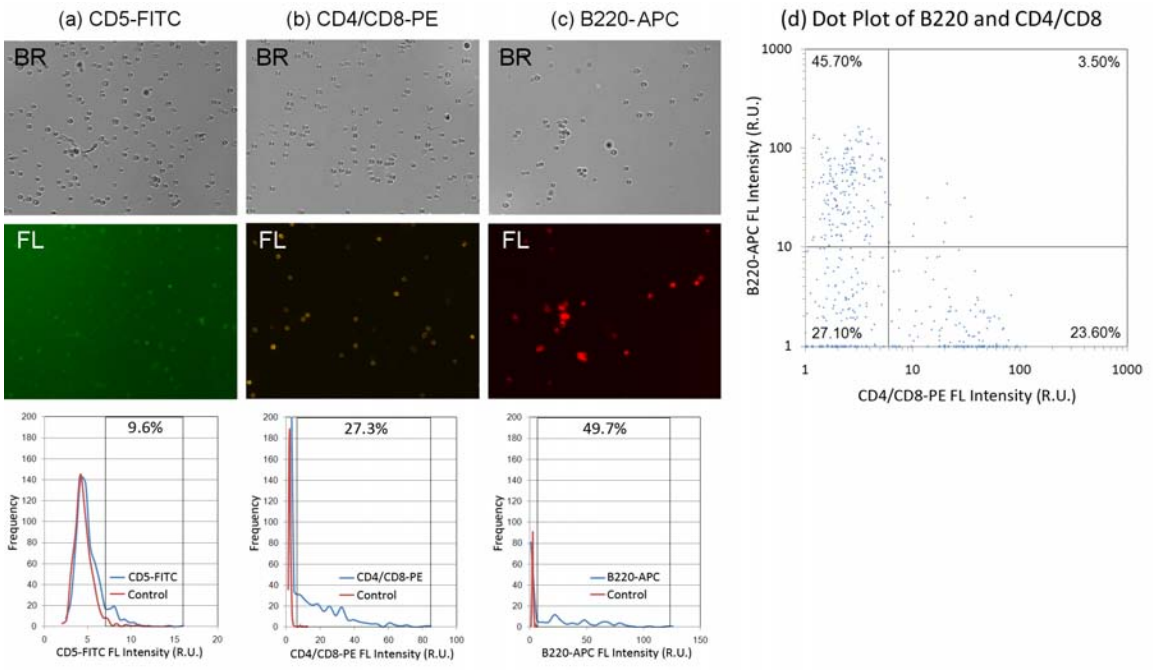

Figure 2. Detection of $CD4^+$ and $CD8^+$ splenocytes and thymocytes.

Analysis of (a) splenocytes and (b) thymocytes stained with anti-CD4 and anti-CD8. Bright-field and fluorescence images of CD4-APC (red) and CD8-PE (yellow) stained splenocytes and thymocytes and overlaid images are shown.

- Cells in circles showed either CD4 or CD8 labeling in splenocytes. Single and double stained cells were observed only in thymocytes (circle).
- The fluorescence histogram of $CD4^+$ and $CD8^+$ on splenocytes and thymocytes are plotted in log scale below the images. (c) Comparison of CD4 and CD8 T cells analysis between Cellometer imaging cytometry method and flow cytometry. CD4 and CD8 T cells were stained with anti-CD4-APC and anti-CD8-PE. Scatter plots (log scale) were generated by Cellometer using fluorescence measurement of CD4 and CD8 labeling (left column).

- Results of flow cytometry analysis were analyzed using FlowJo software and are shown at right column.
- The scatter plot of fluorescent intensities measured using Cellometer was comparable to the flow cytometry results.
- The two distinct $CD4^+$ and $CD8^+$ splenocytes populations detected by Cellometer Vision were similar to that detected by flow cytometry.
- For thymocytes, the percentages of single positive (SP) and double positive (DP) thymocytes were also consistent with the flow data.

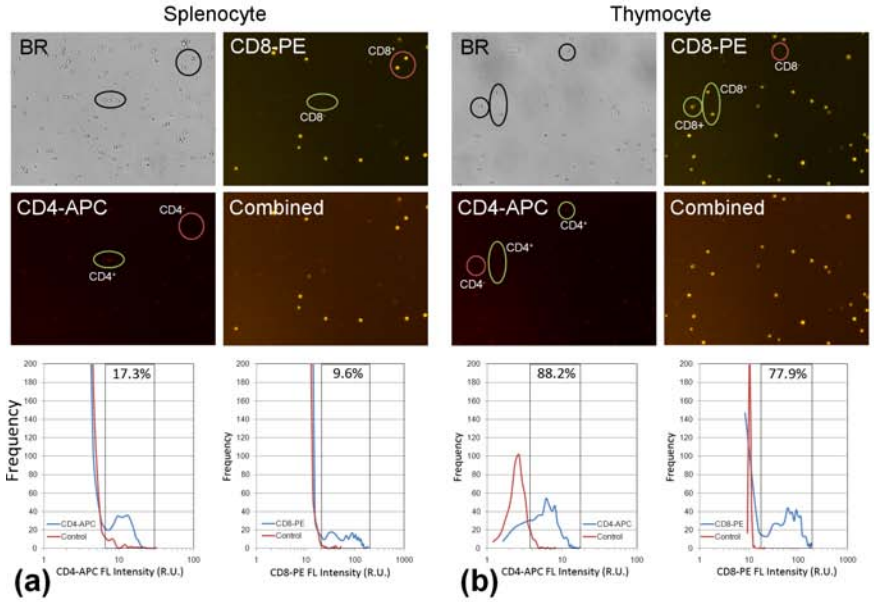

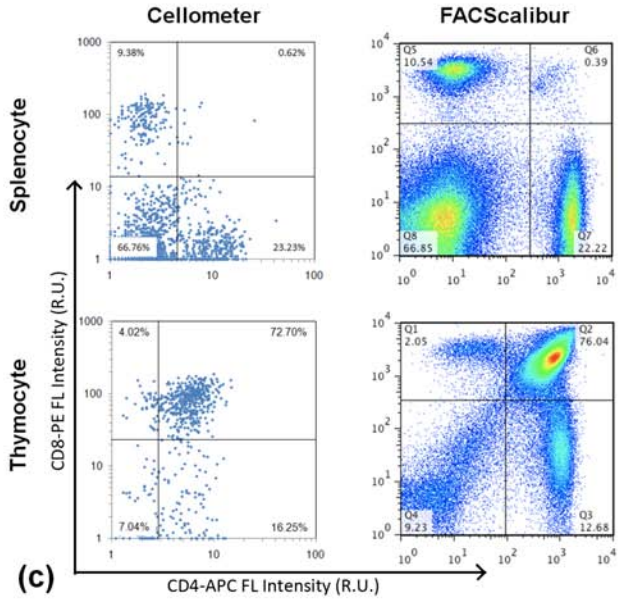

Conclusions

- The ability to rapidly and cost-effectively perform imaged-based immunophenotyping may improve research efficiency, especially where a flow or laser scanning cytometer is not available or in situations where a rapid analysis of data is critical.
- Cellometer Vision performed the immunophenotyping experiments outlined here and achieved results consistent with those of the conventional flow cytometry method.
- Besides the compatibility, Cellometer Vision method also has several advantages over conventional flow cytometry:
    - In comparison to the 300 μL of sample for flow cytometry, only 20 μL of sample is required for the Cellometer Vision. It can immediately provide both concentration and percentage of each cell population, whereas further post-harvest analysis is usually required to obtain flow cytometry results and indirect calculation is needed to obtain cell concentration.
    - In addition, the ability to record both BR and FL images of cell sample allows for visual verification of cell detection and image analysis, which cannot be done by conventional flow cytometry.
    - Also, the counting algorithm enables declustering of clumpy cells, which improves accuracy and consistency of population analysis.
    - Furthermore, the lack of high power lasers or photo-multiplying tubes in the Cellometer systems eliminates the need for precise optical alignment, where the simple epifluorescence setup does not require daily user maintenance.
- Further improvement in instrument sensitivity, counting volume, and higher throughput will make it more versatile in the future.

References

1. D'Archangelo, M., *Flow cytometry: new guidelines to support its clinical application.* Cytometry B Clin Cytom, 2007. **72**(3): p. 209-10.

2. Fenili, D. and B. Pirovano, *The automation of sediment urinalysis using a new urine flow cytometer (UF-100).* Clin Chem Lab Med, 1998. **36**(12): p. 909-17.

3. Ludwig, W.-D. and E. Thiel, *Routine immunophenotyping of acute leukemias.* Ann Hematol, 1990. **60**(1): p. 48-50.

4. Stein, D.S., J.A. Korvick, and S.H. Vermund, *CD4+ lymphocyte cell enumeration for prediction of clinical course of human immunodeficiency virus disease: a review.* J Infect Dis, 1992. **165**(2): p. 352-63.

5. Hystad, M.E., et al., *Characterization of early stages of human B cell development by gene expression profiling.* J Immunol, 2007. **179**(6): p. 3662-71.

6. Reddy, M., et al., *Comparative analysis of lymphocyte activation marker expression and cytokine secretion profile in stimulated human peripheral blood mononuclear cell cultures: an in vitro model to monitor cellular immune function.* J Immunol Methods, 2004. **293**(1-2): p. 127-42.

7. Chan, L.L., et al., *Direct concentration and viability measurement of yeast in corn mash using a novel imaging cytometry method.* J Ind Microbiol Biotechnol, 2011. **38**(8): p. 1109-15.

8. Pirani, A., *Yeast concentration and viability using image-based fluorescence analysis.* Nat Meth, 2010.